International Journal of Nanoelectronics and Materials
IJNeaM
ISSN 1985-5761 | E-ISSN 2232-1535

Influence of Nb-doped Nanoparticles Via the Solvothermal Method on the Performance of Dye-Sensitized Solar Cells

Hidayani Jaafar[a,*], Haryati Jaafar[b], Nadiah Ameram[c], Ashraf Said Almadhoun[d]

[a,c]*Faculty of Bioengineering and Technology, Universiti Malaysia Kelantan, 17600 Jeli, Kelantan, Malaysia*
[b]*Department of Mechatronic, Faculty of Electrical Engineering & Technology, Universiti Malaysia Perlis, Arau, Perlis, Malaysia*
[d]*Gaza Training Community College, Gaza Strip, Palestine*
* *Corresponding author. Tel.: +019-9572010; e-mail: hidayani@umk.edu.my*

Received 16 June 2025, Revised 18 Jan 2026, Accepted 21 May 2026

ABSTRACT

In this study, niobium (Nb) doped TiO_2 nanoparticles, synthesized via the solvothermal method, were utilized to fabricate TiO_2 based dye-sensitized solar cells (DSSCs), with *E. conferta* fruit extract serving as the photosensitizer and ethanol used as the solvent. The synthesized metal oxide semiconductor nanoparticles were characterized using XRD, FESEM, BET, and UV–Vis spectroscopy. The photovoltaic studies, including current density, voltage and factor performance of the cells were analyzed. Based on the analysis conducted in this study, the improvement in cell efficiency indicates that the solvothermal method can be used as one of the fabrication methods due to its simplicity and lower time requirement compared with the sol-gel and solid-state methods. The solvothermal method can also reduce recombination, thereby producing more efficient results than other methods.

Keywords: *Solvothermal method, Nb doped TiO_2, E. conferta, Phase analysis, Photovoltaic parameters*

1. INTRODUCTION

The growing global population each year has made the development of clean and affordable energy sources for research areas increasingly essential. To reduce energy consumption, technologists and researchers are focusing more on meeting energy demands by developing efficient, low-cost devices [1]. Recently, harvesting energy from sunlight through photovoltaic technologies has gained significant attention due to their low cost, high efficiency, and durability [2-3]. The third generation of dye-sensitized solar cells has gained significant attention from researchers in recent decades due to its use of low-cost materials, transparency, and ease of fabrication, making it well-suited for energy development compared to earlier generations of solar cells [4]. DSSC photoanode fabricated with a transparent conducting oxide substrate that is coated with wide band gap materials and immersed in sensitised dye [5]. TiO_2 is the preferred semiconductor material due to its excellent optical properties and high photostability. Various approaches have been explored to modify the structure of photoanode materials to optimise DSSC performance, such as doping TiO_2 with metal ions. Acceptor dopants such as niobium, vanadium, iron, copper, and zinc have been incorporated into TiO_2 to fabricate the photoanode of DSSCs [6-11].

In this study, Nb doping is applied to TiO_2 nanoparticles, as Nb is considered one of the most promising metal dopants for enhancing optical properties. Doping the TiO_2 semiconductor in DSSCs offers three main advantages: it reduces the band gap to enhance efficiency, decreases the photocatalytic activity of the cell, and minimizes charge recombination. Doping with metals with higher valency than Ti^{4+}, such as Nb^{5+}, offers several benefits, including increased free charge carriers, improved electrical conductivity, enhanced charge-transfer kinetics, and modified dye absorption properties in TiO_2. Previous research on niobium (Nb)-doped TiO_2 using the co-hydrolysis method observed enhanced electron injection and transport, attributed to increased electrical conductivity and shifts in both the Fermi level (E_n) and the conduction band minimum (CBM) [12-13].

However, achieving high crystallinity and uniform particle size with the co-hydrolysis method is challenging, and the process often introduces structural defects in TiO_2, which negatively impact electron injection and transport [14]. Doping via the co-hydrolysis method often yields deep dopant energy levels that are ineffective for electron injection and transport. Extensive research has been conducted on the photovoltaic performance of Nb-doped TiO_2 photoanodes; however, their fabrication via the solvothermal method has not yet been reported. Nb doped TiO_2 synthesized using the solvothermal method often exhibits distinct advantages in terms of morphological control, particle dispersion, and enhanced surface area compared to those prepared by sol–gel and solid-state methods. In solvothermal synthesis, the high-pressure and moderate-temperature conditions promote uniform nucleation and crystallite growth, resulting in smaller crystallite sizes, improved homogeneity, and higher surface areas. Enhancing dye adsorption and charge transportation contributes to higher DSSC performance. Sol-gel technique can produce more uniform nanostructure; however, the addition of a calcination step can decrease the surface area and grain growth and affect the properties of DSSC [15]. Crystallite sizes obtained through the sol–gel method generally fall within the range of 15–30 nm, while the surface area tends to be slightly reduced because of particle agglomeration [16]. High-temperature dry-mixing process in solid state method produces larger crystallite size and form agglomeration between particles and causes lower surface area and less Nb dispersion [17]. The solvothermal method can control light absorption due to effective Nb dispersion within the TiO_2 lattice. Benefits of using solvothermal include more efficient transport, lower recombination, and increased light-harvesting capability.

In this research, Nb-doped TiO_2 photoanode synthesis using the solvothermal method, in combination with *E. conferta* as natural dyes as sensitisers. *E. conferta* was selected due to high anthocyanin pigments that enhanced the conversion of photons to electrical energy [18]. By using the solvothermal method, pH adjustment, strict temperature control, and complex chemical preparations can be removed from the fabrication process and reduce time consumption for the synthesis of Nb-doped TiO_2. These benefits promote more efficient electron injection and transport, resulting in enhanced photovoltaic performance.

2. EXPERIMENTAL METHODS

2.1 Nb Doped TiO_2 Nanoparticles Synthesis

6 mL of titanium isopropoxide was mixed with 12 mL acetic acid for undoped TiO_2 using solvothermal method. 12 mL ethanol was mixed in the mixture and stirred for 2 hours. The solution was put in Teflon-lined autoclave and heated 200°C for 90 minutes. Once cooled to room temperature, the product was filtered, rinsed with ethanol, and subsequently dried at 80°C for several hours. Meanwhile, preparation of Nb-doped TiO_2 prepared same procedure as TiO_2 but blended with $NbCl_5$ with 30 minutes continuously. Nb doped varies from 0, 0.5, 1.0 and 1.5 wt%, respectively with same process.

2.2 Natural Dye Preparation

E. conferta fruits was used in this research as natural dye. Flesh and seed were separated and dried at room temperature. By sing mortar, dried flesh was ground until fine powder was formed. 50 g of this powder were placed in a beaker, combined with 500 mL of ethanol at a 1:10 ratio, and thoroughly stirred and left the mixture for 24 hours in dark condition. Afterward, the mixture was filtered to remove residues and obtain natural dye solution with one time purification. Details of natural dye can be found in our previous research [19].

2.3 DSSC Assembly

7 Ω/cm^2 of FTO glass was cleaned using ethanol before applied with Nb-doped TiO_2 paste. 0.3 g of TiO_2 mixed with 0.5 mL of acetic acid with 1:1 DI water and ethanol and stirred for 20 minutes to prepare the paste. During stirred process, 0.5 mL triton X was added enhancing the bounding between photoanode paste. The TiO_2 paste was spread onto the FTO glass using the doctor blade method, and the coated films were then sintered at 450°C for 30 minutes. Nb-doped TiO_2 films with doping levels of 0.5 wt%, 1.0 wt%, and 1.5 wt% were prepared using the same procedure and immersed in for 24 hours. Following sensitization, the electrodes were washed with ethanol to eliminate any unbound dye. The counter electrode was fabricated following the procedures outlined in previous studies [20]. Redox electrolyte was applied in between photoanode and counter electrode and ensure that electrolyte cover active area in photoanode and counter electrode. Next, the cell was sealed with slurry tape with active area of cell is 7 cm^2.

3. RESULTS AND DISCUSSION

Crystal structure properties including lattice strain and crystallite size were discussed in this section. Absorption of visible light in order to determine the effectiveness of photon absorbance was investigated using UV-VIS. Meanwhile, scanning electron microscopy (SEM) used for morphological identification, revealing their polycrystalline nature. EIS was conducted to study the recombination characteristics and lastly, performance of Nb doped TiO_2 using solvothermal method was investigated through photovoltaic performance.

3.1. XRD Analysis

Pure TiO_2 and Nb-doped TiO_2 nanoparticles) was shown in Figure 1. These diffraction peaks correspond to the reflections of the anatase phase and align well with JCPDS File No 98-004-5316. In Figure 4.10(a), lattice distortions caused by defects such as vacancies, interstitials, and substitutions can lead to shifted of peak whether strain that present in the composition were tensile or others. To assess changes in the crystal lattice parameters, the (101) peak at 25.3° of Nb-doped TiO_2 was examined as shown in Figure 1(b). The enlarged image shown in Figure 1(b) reveals shifts in peak positions and changes in peak broadening. From 0.5 wt% onwards, peaks were shifted to right indicated that Nb was occupied into TiO_2 lattice and disturbed the structure. Even though the peaks were shifted to the right angle, anatase structure is present and there is no evidence of phase of dopant related in the XRD result. The ionic radius of Nb^{5+} is significantly larger than that of Ti^{4+}. Lattice distortion was occurred due to ionic radius of Nb^{5+} (0.78 Å) is bigger than Ti^{4+} (0.75 Å) and expansion of crystallite size can be seen from Table 1 [21]. Nb^{5+} preferentially occupies the octahedral interstitial site due to energetic favorability. The incorporation of Nb^{5+} is beneficial as it donates electrons to TiO_2, thereby enhancing its n-type characteristics. Therefore, using a substituent with a higher valence electron count than Ti^{4+}, such as Nb^{5+}, is considered an effective approach to modifying the electronic properties of TiO_2.

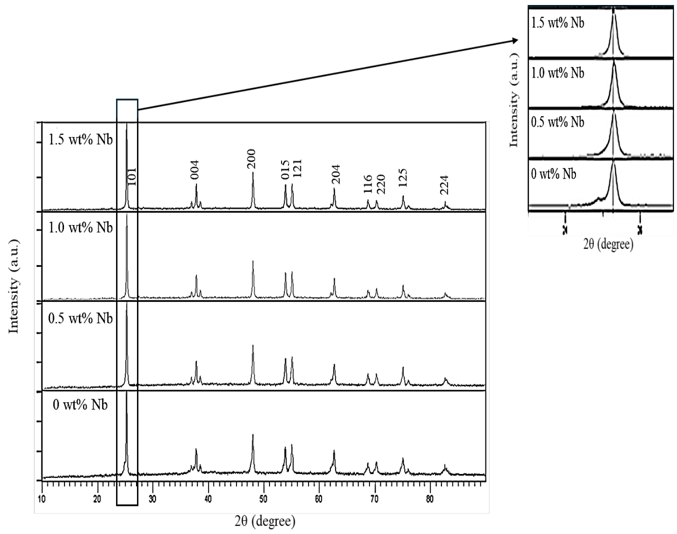

Figure 1. (a) Pure oiO$_2$ and different amounts of Nb (b) an enlarged view of the (101) peaks for undoped TiO$_2$ and Nb-doped TiO$_2$.

The impact of dopants on lattice constants is shown in Table 1. Based on the Table 1, when doped with NB, the length between Ti and O bond were increased due to rises of cell volume and length of Nb with O getting longer compared to Ti and O. This leads to an expansion of the unit cell volume in doped TiO$_2$, accompanied by the emergence of a local strain field at the dopant sites and modify atomic interactions and induce lattice distortion [22-23]. Thus, notable changes in crystal parameters were observed as Nb content increased, as reflected in analyses of lattice constants and crystallite sizes. Additionally, the broadening of the full width at half maximum (FWHM) in the XRD patterns decreases with increasing Nb doping concentration, which is attributed to the growth in crystallite size. This is attributed to the expansion of Nb-doped TiO$_2$ samples, resulting from the incorporation of Nb^{5+} ions into interstitial positions within the TiO$_2$ lattice [24]. The lattice constants (a and c) and the cell volume expand with increasing Nb content. Consequently, increasing Nb content leads to notable changes in crystal parameters, as shown by analyses of the lattice constant and crystallite size, which subsequently influence DSSC performance.

Table 1 Analysis based on peak (101) for pure and doped TiO$_2$

Sample	Crystallite size (nm)	(Å^3)	*a* (Å)	*c* (Å)
Pure TiO$_2$	9.00	140	3.80	10.50
0.5 Nb doped TiO$_2$	9.16	146	3.81	10.51
1.0 Nb doped TiO$_2$	12.00	146.3	3.81	10.51
1.5 Nb doped TiO$_2$	12.10	146.4	3.85	10.52

By comparing with another fabrication method such as sol-gel, hydrothermal and solid state, solvothermal is able to produce a small crystallite size (between 8 and 11 nm) compared to others (20-25 nm for sol-gel and solid state, more than 30 nm) [25-26]. Therefore, fine control of crystallite size allows better electron diffusion.

3.2. UV-VIS Analysis

To investigate the behavior and understand the photoanode characteristics, optical analysis was conducted as shown in Figure 2. As observed, the range of 350 to 420 nm showed the strongest photon absorbance for Nb concentrations. The absorption wavelength increases with increasing N- doping concentration up to 1.0 wt%, which is attributed to the formation of new conduction bands or the creation of new energy levels within the TiO$_2$ structure [27]. Furthermore, increasing the Nbn doping concentration to 1.5 wt% leads to a decrease in the optical absorption wavelength. Higher energy values indicate the Nb substituted into the TiO$_2$ lattice due to movement of band gap to another level. This shows that dopants introduced can modify the energy of the optical bandgap. The enhanced absorption may be attributed to a new energy level introduced between the conduction and valence bands, which leads to a slight reduction in the band gap and, consequently, a redshift in light absorption. The decrease in absorbance at 1.5 wt% Nb is attributed to degradation of crystal quality, which increases photon scattering, as observed in the XRD results [28]. This can be observed in Figure 1 where XRD peak broadening indicates increased lattice strain. Degraded crystallinity reduces the mean free paths of photons and electrons, which can affect both electrical and optical properties. With degraded crystallinity at 1.5 wt% Nb, optical absorbance decreases due to Increased recombination centers, which diminish photo-generated charge carriers.

Based on equation 1, the optical band gap of Nb-doped TiO2 can be determined together with the Tauc plot.

$$\alpha h v = A(h v - E_g)^n \quad (1)$$

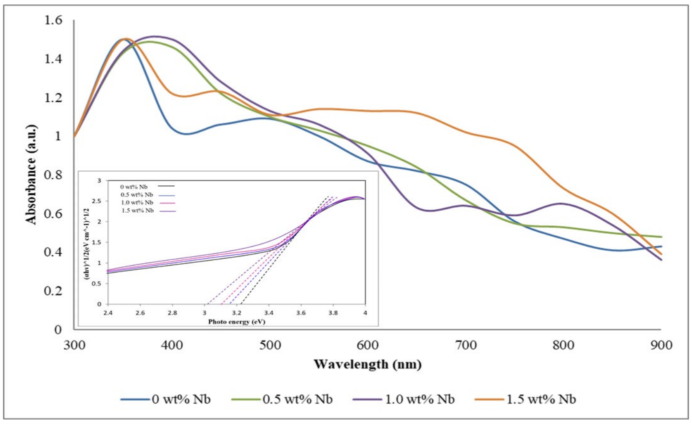

Figure 2. Analysis of UV–vis photon absorbance for pure and doped TiO2.

The energy band gap decreases as the dopant concentration increases. Notably, the band gap can be effectively tuned to a desired level by selecting the appropriate doping concentration of transition-metal ions in the host TiO2, thereby shifting the optical absorption edge from the UV to the visible region [29]. A reduction in the band gap creates new electronic states within the material. The reduced band gap improves electron transport and enhances the performance of Nb-doped TiO2 in DSSCs.

The solvothermal method can enhance Nb incorporation andopticale absorption in Nb-doped TiO_2 compared to the sol–gel and solid-state methods [30–31]. By doping with Nb via solvothermal, light absorption can be enhanced with the narrowing of the band gap compared to the sol-gel and solid-state methods, which have a tendency to widen the band gap and decrease the efficiency of electron transporting.

3.3. FESEM Analysis

Figure 3 shows the surface morphology of the samples obtained by solvothermal synthesis. Small agglomeration of samples 0 wt% and 0.5 wt% Nb. However, at samples 1.0 wt% and 1.5 wt% Nb, continuous and dense particles with small porosity were produced. At 1.0 wt% and 1.5 wt%, the surface tends to form a denser and smoother surface compared to 0 wt% and 0.5 wt% Nb. Better dye penetration in the photoanode and more efficient electron injection with the presence of pores [32]. Effective pore penetration decreased with presented of smaller particles due to more tighter spacing between each particle. The reason is that it can reduce electron transport from the electrolyte to the photoanode, enhance recombination centres, and reduce the cell's effectiveness.

Particle sizes and porosity were measured using ImageJ software. As shown in Table 2, the grain size decreased from 131.3 nm to 126 nm when the Nb content increased from 0 wt% to 1.0 wt%. However, it then increased to 128.5 nm at 1.5 wt% Nb. A similar trend was observed for porosity: an increase in particle size led to a decrease in porosity.

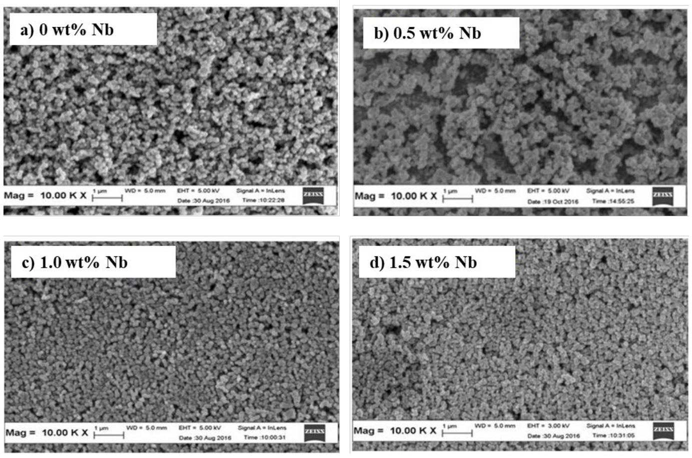

Figure 3. FESEM images of pure and doped TiO_2 at varying Nb concentrations.

This is attributed to the formation of new nucleation centers, enhancing the heterogeneous nucleation process at preferential sites such as phase boundaries or impurities. The dopant atoms hinder the growth of TiO_2 crystals due to their interaction with Ti^{4+}, thereby slowing down the crystal growth [33]. Further doping with Nb increased particle size due to agglomeration and decreased porosity. The doping of TiO_2 with large cations like Nb can be understood by considering that if these large dopants substitute Ti, the segregated TiO_2 may form a liquid phase. This liquid phase could then facilitate grain growth during the subsequent addition of dopants. Agglomeration of Nb-doped TiO_2 tends to occur as Nb concentration increases, leading to larger particle size and reduced porosity. This occurs because Nb acts as a defect, preventing the dye from binding to the Nb-doped TiO_2 photoanode. The presence of Nb at or near the surface changes the surface chemistry of TiO_2. Nb can occupy active sites or introduce competing bonding sites, preventing effective dye attachment. Therefore, Nb doping can also alter the surface energy levels of TiO_2, possibly changing how the dye interacts electronically with the surface and affecting electron injection and anchoring.

Table 2 FESEM Analysis

Sample	Grain size (nm)	Porosity (%)	Surface area (m^2/g)
0 wt% Nb	131.3	75.06	6.1407
0.5 wt% Nb	126.5	75.13	-
1.0 wt% Nb	126.0	75.16	8.8314
1.5 wt% Nb	128.5	75.12	7.3451

3.4. DSSC Photovoltaic Performance

Figure 4 shows the photovoltaic performance of short circuit current density and open circuit current voltage, and Table 3 summarises the analysis from m Figure 4. The addition of Niobium enhanced the properties of the photovoltaic cells. However, below a certain amount, the properties will decrease due to an excessive number of dopants that boost the cell's performance. The highest result was obtained with 2.50% cell performance. The increased J_{SC} reflects enhanced electron injection and transport, attributed to improved cell conductivity and the introduction of a new energy level that facilitated more efficient electron transfer. This can be correlated with the reduction in the band gap in section 3.2. By creating a new energy level, more free electrons were introduced into the valence band and were excited to jump to the new level without losing energy. Therefore, higher J_{SC} can be obtained, and more efficient cells can be created with these solvothermal processing techniques due to an increase in carrier in the new energy level that is created near the conduction band. Correlation can also be observed in Table 2, where smaller grain sizes increased the nanoparticles' surface area, leading to greater dye absorption by the photoanodes. The more absorption, the more $J_{SC,}$ which boosts DSSCe efficiency. The decrease in J_{SC} is attributed to the oxidation of Nb, which introduces new recombination centres (electron recombination reactions at the photoanode/dye/electrolyte interface). This process reduces the number of charge carriers, leading to a lower J_{SC} value as shown in 1.5 wt% Nb [34].

Meanwhile, the increase in V_{OC} can be attributed to the enhanced optical absorption. Nb can act as a suppressing agent that decreases the charge recombination and at the same time increases the value of $V_{OC.}$ A new energy level between the conduction and valence bands was introduced, which suppressed recombination centres between the bands, thereby improving electron mobility without jumping into recombination sites. Therefore, Nb dopants create an energy level that can improve photovoltaic properties, even when a natural dye is used in this study. Nb doping enhances the photo response by introducing additional energy levels within the TiO_2 band gap. Consequently, the internal resistance decreases due to the modified electronic structure of TiO2. The J_{SC} and V_{OC} of DSSCs are significantly influenced by the synthesis method of Nb-doped TiO_2. Among the common fabrication methods, the solvothermal, sol–gel, and solid-state methods, the solvothermal method generally yields superior photovoltaic performance. This is primarily due to its ability to produce well-crystallized nanoparticles with smaller and more uniform particle sizes, typically in the range of 8–11 nm, along with a higher surface area and porosity [25-26]. These characteristics enhance dye adsorption, facilitate better electrolyte infiltration, and improve electron transport, resulting in higher J_{SC} values, typically around 5.20–6.00 mA/cm2. Higher V_{OC} in the range 0.4-0.5 V due to improvement of crystallinity and defect reduction, which helps to suppress recombination of charge in the photoanode.. Compared with the sol-gel and solid-state methods, the solvothermal method was more efficient at producing higher $V_{OC\ levels}$ due to uniform particle sizes and a higher surface area [35]. Even though solid-state method offers simpler and cost-effective, high tendency for particles agglomeration and low surface area decreased the dye loading and limit the electron transportation and decreased the performance of photovoltaic [36]. Consequently, DSSCs fabricated via the solid- state route typically exhibit the lowest JSC (0.2–2.29 mA/cm2) and VOC (0.28–0.5 V) among the three methods [36]. Overall, the solvothermal method provides a more favorable nanostructure and electronic environment, making it the most effective approach for enhancing the JSC and VOC performance of Nb-doped TiO2-based DSSCs.

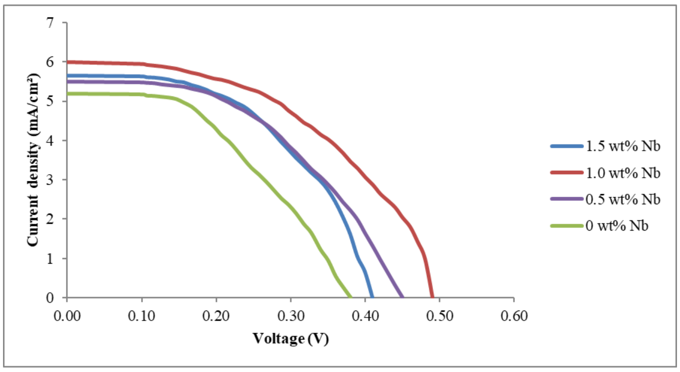

Figure 4. Performance of photovoltaic based on short circuit current density and open circuit current voltage for all samples using solvothermal method.

Table 3 Analysis of photovoltaic performance for all samples using solvothermal method

Sample	J_{SC} (mA/cm²)	V_{OC} (V)	FF	η (%)
0 wt% Nb	5.20	0.38	0.78	1.54
0.5 wt% Nb	5.65	0.45	0.80	2.03
1.0 wt% Nb	6.00	0.49	0.85	2.50
1.5 wt% Nb	5.71	0.41	0.80	1.87

4. CONCLUSION

The successful synthesis of Nb-doped TiO_2 nanoparticles via the solvothermal method and their integration into dye-sensitized solar cells (DSSCs) using E. conferta fruit extract as a natural sensitizer highlight a promising approach for low-cost, eco-friendly photovoltaic devices. Structural analysis via XRD confirms the formation of a hexagonal TiO_2 phase with nanoscale crystallinity, while UV–Vis and Tauc analysis reveal a systematic reduction in bandgap with increasing Nb content, indicative of enhanced visible-light absorption. Notably, the DSSC fabricated with 1.0 wt% Nb-doped TiO_2 achieved a peak power conversion efficiency (PCE) of 2.50%, along with a Voc of 0.49 V and Jsc of 6 mA/cm^2, outperforming other doping levels. Nb doping can tune the electronic structure and electron transport to improve the performance of DSSCs. Combination with natural dyes can also enhance performance due to more effective molecular bonding with Nb-doped TiO2 photoanode and produce sustainability to the environment. In this research, not only does understanding metal oxide modification tune the properties of DSSC, but it also helps us develop more environmentally friendly approaches for the next generation of solar cells.

ACKNOWLEDGMENTS

Credit to Fundamental Research Grant Scheme (FRGS), Malaysia, under grant number FRGS/1/2023/TK08/UMK/02/1.

REFERENCES

[1] A. Ali, S.A. Hassan, A. BaQais, J.S. Binoj, P. Velmurugan, A Study on the Application of Solar Cells Sensitized with a Blackberry-Based Natural Dye for Power Generation, J. Nanomater. 2022 (2022) 1–10.

[2] S. Al Batty, S.M. Al-Jubouri, M. Wali Hakami, A. Sarief, SK.M. Haque, Innovative economic anthocyanin dye source for enhancing the performance of dye-sensitized solar cell, Journal of Taibah University for Science 16 (2022) 415–422.

[3] E. Selva Esakki, L. Renuga Devi, Devi, S. Meenakshi Sundar, Fabrication of Dye- Sensitized Solar Cells Using Aqueous and Ethanolic Extracts of Ixora macrothyrsa Flowers, Applied Biological Research. 24 (2022) 184-190.

[4] T.G. Vignesh Prabhu, J. Chandrasekaran, D. Thangaraju, P. Vivek, S. Gopi, Fabrication and performance analysis of set standard natural dye-sensitized solar cell (N-DSSC) using extracted Terminalia kattapa (Red), Azadirachia indica (Green), and Clitoria ternatea (Blue) dyes with virgin Degussa p25 photo-anode, J. Mater. Sci. Mater. Electron. 33 (2022) 17331–17342.

[5] K. Magiswaran, M.N. Norizan, I.S. Mohamad, N. Mahmed, S.N. Idris, S.A. Sobri, Charge Recombination in Zinc Oxide-Based Dye-Sensitized Solar Cell: A Mini Review, Int. J. Nanoelectron M. 14 (2021) 59-66.

[6] T.G. Vignesh Prabhu, J. Chandrasekaran, D. Thangaraju, P. Vivek, S. Gopi, Fabrication and performance analysis of set standard natural dye-sensitized solar cell (N-DSSC) using extracted Terminalia kattapa (Red), Azadirachia indica (Green), and Clitoria ternatea (Blue) dyes with virgin Degussa p25 photo-anode, J. Mater. Sci. Mater. Electron. 33 (2022) 17331–17342.

[7] R.T. Ako, P. Ekanayake, A.L. Tan, D.J. Young, La modified TiO_2 photoanode and its effect on DSSC performance: A comparative study of doping and surface treatment on deep and surface charge trapping, Mater. Chem. Phys. 172 (2015) 105–112.

[8] O. Kalu, M.R. Correia, A. Cantarero, H.A. Martinez-Rodriguez, J.A. Duarte-Moller, A. Reyes-Rojas, Enhanced optical properties of Cd–Mg-co-doped ZnO nanoparticles induced by low crystal structure distortion, J. Phys. Chem. Solid 146 (2020) 109611.

[9] R. Sarathi, N.L. Sheeba, E. Selva Essaki, S.M. Sundar, Titanium doped Zinc Oxide nanoparticles: A study of structural and optical properties for photocatalytic applications, Mater. Today:. Proc. 64 (2022) 1859–1863.

[10] A.H. Ghanbari Niaki, A.M. Bakhshayesh, M.R. Mohammadi, Double-layer dye sensitized solar cells based on Zn-doped TiO_2 transparent and light scattering layers. Sol Energy 103 (2014) 210–22.

[11] X.D. Li, X.J. Han, W.Y. Wang, X.H. Liu, Y. Wang, X.R. Liu, Synthesis, characterization and photocatalytic activity of Nb-doped TiO_2 nanoparticles. Adv Mater Res 110 (2012) 455–456.

[12] N. Kanjana, W. Maiaugree, P. Poolcharuansin, P. Laokul, Size controllable synthesis and photocatalytic performance of mesoporous TiO_2 hollow spheres. J. Mater. Sci. Technol. 48 (2020) 105–113.

[13] C.A. Stevenson, J.E. Monroe, C.G. Norris, A.R. Roginski, S.P. Beaudoin, The effects of surface and particle properties on van der Waals (vdW) adhesion quantified by the enhanced centrifuge method. Powder Technol. 392 (2021) 514–523.

[14] L. De Trizio, R. Buonsanti, A.M. Schimpf, A. Llordes, D.R. Gamelin, R. Simonutti, D.J. Milliron, Nb-Doped colloidal TiO_2 nanocrystals with tunable infrared absorption. Chem. Mater. 25 (2013) 3383–3390.

[15] J. Liu, X. Zhao, L. Duan, M. Cao, H. Sun, J. Shao, S. Chen, H. Xie, X. Chang, C. Chen, Influence of annealing process on conductive properties of Nb-doped TiO2 polycrystalline films prepared by sol–gel method, Appl. Surf. Sci. 257 (2011) 10156–10160.

[16] M. Duta, L. Predoana, J.M. Calderon-Moreno, S. Preda, M. Anastasescu, A. Marin, I. Dascalu, P. Chesler, C. Hornoiu, M. Zaharescu, P. Osiceanu, M. Gartner, Nb-doped TiO2 sol–gel films for CO sensing applications, Mater. Sci. Semicond. Process. 42 (2016) 397–404.

[17] D. Sinha, D. De, A. Ayaz, Performance, and stability analysis of curcumin dye as a photo sensitizer used in nanostructured ZnO based DSSC, Spectrochim. Acta A. 193 (2018) 467–474.

[18] E.S. Esakki, R. Sarathi, S.M. Sundar, L.R. Devi, Fabrication of Dye Sensitized Solar Cells using Ixora Macrothyrsa. Mater. Today:. Proc. 47 (2021) 2182–2187.

[19] H. Jaafar, M.F. Ain, Z.A. Ahmad, Performance of E. conferta and G. atroviridis fruit extracts as sensitizers in dye-sensitized solar cells (DSSCs). Ionics 24 (2018) 891-899.

[20] H. Jaafar, M.F. Ain, Z.A. Ahmad, The use of carbon black-TiO_2 composite prepared using solid state method as counter electrode and E. conferta as sensitizer for dye-sensitized solar cell (DSSC) applications. Ot. Mater. 79 (2018) 366-371.

[21] P. Zhong, X. Chen, B. Niu, C. Li, Y. Wang, H. Xi, Y. Lei, Z. Wang, X. Ma, Niobium doped TiO2 nanorod arrays as efficient electron transport materials in photovoltaic. J. Power Sources 450 (2020) 227715.

[22] A. Prasad, F. Singh, V. Dhuliya, L.P. Purohit, R.C. Ramola, Structural and optical characteristics of Cr-doped TiO_2 thin films synthesized by sol-gel method. Opt. Mater. 151 (2024) 115411.

[23] B.R. Koo, D.H. Oh, H.J. Ahn, Influence of Nb-doped TiO_2 blocking layers as a cascading band structure for enhanced photovoltaic properties. Appl. Surf. Sci. 433 (2018) 27–34.

[24] Y. Horie, K. Daizaka, H. Mukae, S. Guo, T. Nomiyama, Enhancement of photocurrent by columnar Nb-doped TiO_2 compact layer in dye sensitized solar cells with low temperature process of dc sputtering. Electrochim. Acta 187 (2016) 348–357.

[25] S.G. Kim, M.J. Ju, I.T. Choi, H.K. Kim, Nb-doped TiO2nanoparticles for organic dye-sensitized solar cells. RSC Advances 3 (2013) 16380-16386.

[26] M. Yang, D. Kim, H. Jha, Nb doping of TiO2 nanotubes for an enhanced efficiency of dye-sensitized solar cells. Chem. Commun 47 (2011) 2032-2034.

[27] N. Sriharan, T.S. Senthil, P. Soundarrajan, M. Kang, Surface modification of TiO_2 nanorods with Mg doping for efficient photoelectrodes in dye sensitized solar cells. Appl. Surf. Sci. 585 (2022) 152719.

[28] S.K. Nikhil, G.R. Nair, M. Kumar, M. Bhagavathiachari, R.G. Nair, A doped heterojunction photoanode: a strategy-driven approach to improve the charge carrier dynamics and photoconversion performance of the TiO_2-based dye- sensitized solar cell. J. Mater. Sci. Mater. Electron. 35 (2024) 602.

[29] L. Fiter, S. Shafie, Y. Sulaiman, Performance boost of dye-sensitized solar cell by using barium titanate as a compact layer. Opt. Mater. 148 (2024) 114934.

[30] N. Kutlu, C. Zafer, N. Ozek, Analyzing of DSSCs Fabricated by Nb:TiO2 Characterized and Synthesized with Sol–Gel in the Magnetic Field. J Electron Mater. 48 (2019).

[31] D.Y. Lee, J.H. Park, Y.H. Kim, M.H. Lee, N.I. Cho, Effect of Nb doping on morphology, crystal structure, optical band gap energy of TiO2 thin films, Curr. Appl. Phys. 14 (2014) 421–427.

[32] J. Song, Y. Gu, Z. Lin, J. Liu, X. Kang, X. Gong, P. Liu, Y. Yang, H. Jiang, J. Wang, S. Cao, Z. Zhu, H. Peng, Integrating light diffusion and conversion layers for highly efficient multicolored fiber-dye-sensitized solar cells. Adv. Mater. 36 (2024) 2312590.

[33] A.G. Dhodamani, K.V. More, S.M. Patil, A.R. Shelke, S.K. Shinde, D.-Y. Kim, S.D. Delekar, Synergistics of Cr (III) doping in TiO_2/MWCNTs nanocomposites: Their enhanced physicochemical properties in relation to photovoltaic studies. Sol. Energy 201 (2020) 398–408.

[34] P. Huang, S.J. Xu, M. Zhang, W. Zhong, Z. Xiao, Y.P. Luo, Lotus leaf derived natural dye as sensitizer and biochar as counter electrode for dye-sensitized solar cells. MSF 993 (2020) 884–892.

[35] Y. Singh, H. Patel, A. Rai, S. Singh, Bio-capped synthesis of TiO2 nanoparticle using Murraya koenigii leaf extract via ultrasonication assisted sol-gel method and its advanced DSSC performance. Next Materials 8 (2025) 100680.

[36] A. Tiwari, S. Sharma, N. Srivastav, Comparative study of natural dyes extracted from dark red and yellow Frangipani flowers (Plumeria rubra L.) as DSSC sensitizer. Optik 317 (2024) 172055.